

## Structure and Behavior of Regenerated Spider Silk

Zhengzhong Shao,<sup>\*,†,§</sup> Fritz Vollrath,<sup>‡,§</sup> Yong Yang,<sup>†</sup> and Hans C. Thøgersen<sup>‡</sup>

Department of Macromolecular Science and the Key Laboratory of Molecular Engineering of Polymers, Fudan University, Shanghai 200433, People's Republic of China; Department of Zoology, University of Oxford, South Parks Road, Oxford OX1 3PS, UK; Department of Zoology, University of Aarhus, Universitetsparken B135, 8000 Aarhus C, Denmark; and Laboratory of Gene Expression, University of Aarhus, Gustav Wieds Vej 10, 8000 Aarhus C, Denmark

Received September 12, 2002

**ABSTRACT:** Molecule chains of spider silk protein readily self-assemble into ordered structure such as  $\beta$ -sheets when a filament is pulled away from dilute aqueous solution of spider major ampullate silk protein. There is no need to change the pH, the temperature, or the ionic strength of the solution to aid filament formation. Circular dichroism spectroscopy confirmed that the silk protein in such aqueous solution was initially in random coil formation but with time would transform to  $\beta$ -sheets; the process was temperature-dependent. Amino acid analysis showed that reassembled (regenerated) and native spider silks were similar in composition. The morphology and structure of the reassembled silk were investigated by scanning electron microscopy and Raman spectroscopy. The mechanical properties of the reassembled silk were studied in some detail. Our study indicates that reconstituted spider silk self-assembles into respectable filaments. However, it is clear that the spinning process is crucial for the desirable material properties of native silks.

## Introduction

Spider silks have remarkable mechanical properties by combining high tensile strength with outstanding elongation before breaking.<sup>1</sup> This combination makes many spider silks extremely tough even when compared with most high-performance synthetic materials.<sup>2</sup> These special properties of spider silk are essential for its structural role in a complex web and thus its functional role in ensuring spider survival and reproduction.<sup>3,4</sup> Previous work<sup>5–7</sup> suggests that amino acid sequence and hierarchical structure are important determinants of the mechanical properties of this material, and a number of studies<sup>8–10</sup> aimed to elucidate or model the macro- and microstructures of the silk at different hierarchical levels. Nevertheless, the mechanisms of molecular assembly as well as the detailed microstructure of spider silk still remain unclear.

There is considerable interest in producing artificial silk in vitro for industrial production. As a step toward this goal, Seidel and collaborators<sup>11,12</sup> have reported how regenerated spider silk can be spun from hexafluoro-2-propanol and have discussed the properties and structure of such “artificial” silk. Recently, Lazaris et al.<sup>13</sup> produced soluble recombinant (rc)-dragline silk proteins with molecular masses of 60–140 kDa by expressing in mammalian cells the dragline silk genes (ADF-3/MaSpII and MaSpI) of two spider species and then spun monofilaments from a concentrated aqueous solution of soluble rc-spider silk protein by alcohol coagulation. The spun fibers exhibited toughness and modulus values comparable to those of native dragline silks but with much lower tenacity.

However, as in nature spider silk is spun from water to air, we were more interested in how filaments could

be obtained in air from an aqueous solution and how a simple “spinning” process affects both the secondary (and tertiary) structure of silk assembly and afterward the mechanical properties. Hence, we aimed to dissolve raw silk as thoroughly as possible in aqueous solution and then allow the silk protein to “self-assemble” on the surface of the solution into ordered structure. We demonstrate that it was possible to thus draw-regenerate silk filaments with measurable mechanical properties. Studying such regenerated silk filaments allowed us to explore and compare their structural similarity to native spider silk.

## Experimental Section

**Preparation of Spider Silk.** *Nephila edulis* spiders were kept in the laboratory on a diet of houseflies. Native dragline silk was mechanically reeled onto a microscopy slide from the major ampullate glands at 2 cm/s at room conditions ( $24 \pm 3$  °C and  $25 \pm 3\%$  rh). Of this silk 2 mg was dissolved in 3 mL of 8 M guanidine-HCl (with 50 mM Tris-Cl buffer, pH = 8), well shaken, and incubated overnight at room temperature. The solution was centrifuged at 13 000 rpm for 10 min in an Eppendorf microcentrifuge and the supernatant kept. To extract the guanidine-HCl from the solution, gel filtration (G-25) was carried out using deionized water with a Gilson 203 fraction collector (model 202 with 112 UV/vis detector, 254 nm). The peak fraction of the run solution (containing ca. 0.08% w/w silk protein) was collected and stored at 4 °C for up to 3 days. For “spinning” a drop of this aqueous solution of silk protein was placed on a microscope slide again at room conditions. After about 5 min of drying, a needle gently touched the surface of the solution and then pulled away, rapidly solidifying into a filament. Thus, the fiberlike spider protein (here called drawn-regenerated silk) could be drawn out at reasonable speeds (0.5–1 cm/min) to be collected on a frame to be left to air-dry for further measurements.

**Amino Acid Analysis.** After 0.2 mg sample was hydrolyzed in 6 M HCl, the compositions of native spider silk and regenerated silk were analyzed for their amino acid composition with *o*-phthaldialdehyde (OPA).

**Circular Dichroism (CD) Analysis.** Measurements were taken using a Jasco J-715 spectropolarimeter equipped with a slab (NESLAB RTE-111) and purged with N<sub>2</sub> gas at a flow

<sup>†</sup> Fudan University.

<sup>‡</sup> Oxford University.

<sup>§</sup> Department of Zoology, Aarhus University.

<sup>‡</sup> Laboratory of Gene Expression, Aarhus University.

\* To whom all correspondence should be addressed: e-mail zzshao@fudan.edu.cn.

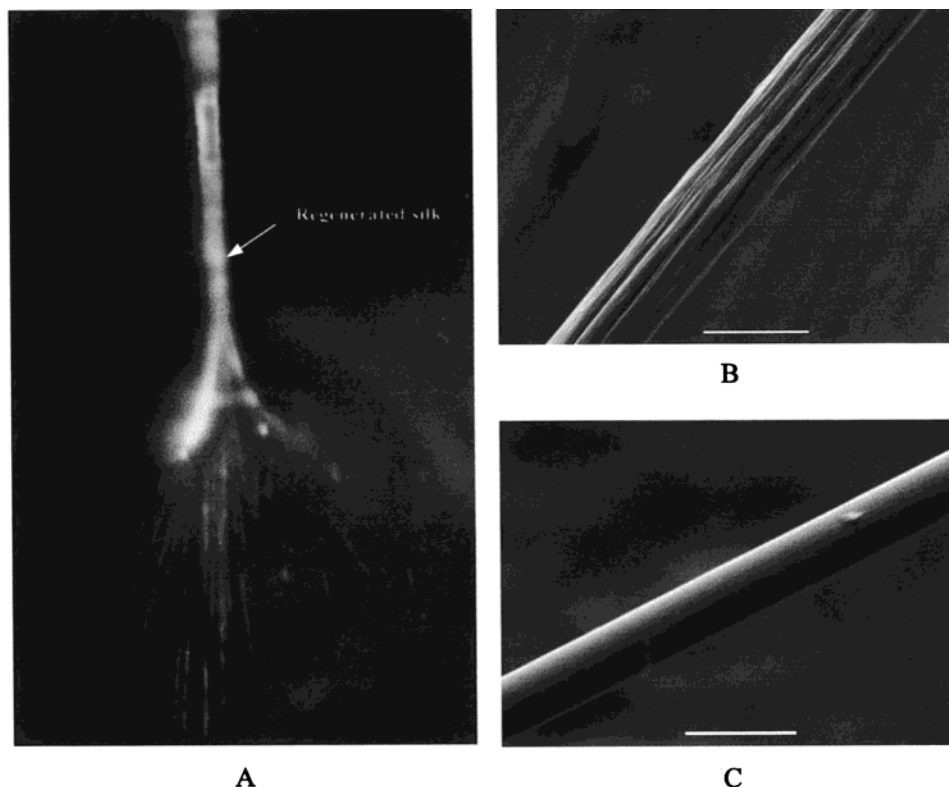


**Figure 1.** Polarizing micrograph of the formation of regenerated silk from aqueous solution (A), SEM micrographs of a regenerated (B, scale bar 12  $\mu\text{m}$ ), and native (C, scale bar 8  $\mu\text{m}$ ) silk fiber from the *N. edulis* spider.

rate of 3–5 mL/min. The aqueous silk protein solution was stored in 0.1 cm path length cells for detection. Spectra were recorded from 190 to 250 nm wavelengths with a resolution of 0.2 nm and an accumulation of six scans. The scan speed was 100 nm/min, and the response time was 0.25 s.

**Scanning Electron Microscopy (SEM).** Taking care to not stretch or otherwise distort the filament, we glued a length of regenerated or native silk fiber onto a SEM stub. The silk was sputtered with gold for 5 min, and its morphology was observed in a CamScan Maxim SEM using an acceleration voltage of 7 kV.

**Raman Spectroscopy.** Spectra were obtained using a Renishaw 1000 Raman microscope from single filaments of regenerated silk or native silk that had been glued onto the appropriate viewing frames. A He–Ne laser was used to give 1 mW of energy at 632.8 nm red line. The laser beam was polarized either parallel or perpendicular to the fiber axis and focused to give a spot size of 2 mm in diameter on the fiber surface. The details of measurement can be found in previous papers.<sup>14,15</sup>

**Mechanical Properties.** The mechanical properties of both regenerated silk and native silk were tested on our custom-built microscale materials testing instrument. The single filament of silks with 12 mm gauge length was fixed between the two hooks of the instrument by using cyanoacrylate instant glue and then was stretched at a rate of 6 mm/min. The controlled environmental conditions in the measuring room were  $25 \pm 2^\circ\text{C}$  and  $50 \pm 5\%$  rh. Technical details can be found elsewhere.<sup>16,17</sup>

## Results and Discussion

**Formation and Texture of Fiber.** Figure 1A shows a regenerated silk filament drawn out from the surface of a 0.08% aqueous solution of regenerated spider silk protein. The filament appears to be “gathered” from a very thin membrane that formed on the surface of the solution. Since 0.08% was a very low concentration of the silk protein solution, we conclude that the molecular chains of the spider silk protein(s) must have the ability

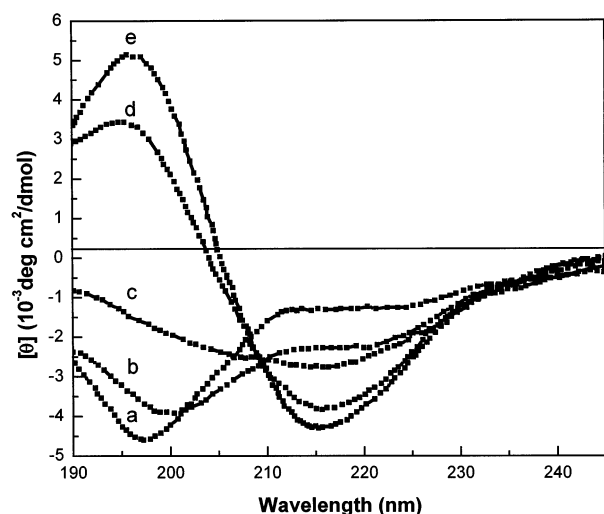
to spontaneously enrich on the surface of this aqueous solution before self-assembling to a membrane.

Compared to the smooth surface of native major ampullate spider silk drawn from the spider (Figure 1C), the regenerated spider silk had a much rougher surface (Figure 1B). Apart from the “wrinkles” along the long axis of the fiber, the surface of the regenerated filament was fairly even and (with an average diameter of about 9  $\mu\text{m}$ ) only slightly thicker than that of native spider silk.

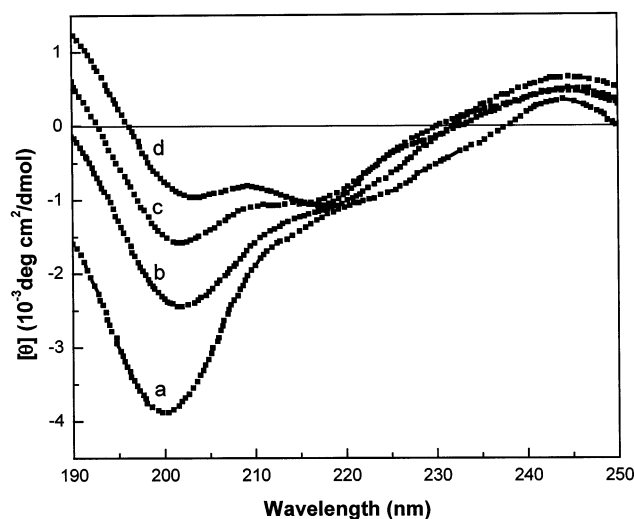
**Amino Acid Compositions of Native Silk and Regenerated Silk.** A chemical composition study of the native spider silk showed that more than 99% of the dragline silk was composed of protein, in which glycine, alanine, and glutamine were the predominant constituents. Table 1 compares the results of our analyses of the amino acids found in both native and regenerated major ampullate silks of *Nephila edulis* with those reported in the literature on native major ampullate silks of the congeneric *N. clavipes*. Clearly, there was little difference in the amino acid compositions for the MA silk of both spiders with the possible exception of proline. The amino acid compositions of our native and regenerated *N. edulis* silks, however, were nearly identical. This would confirm the view<sup>18</sup> of that the high concentration of our solvent guanidine hydrochloride did little more to the silk than disrupt the noncovalent interaction in the proteins. Thus, we may assume that the primary structure of the fibrous silk proteins experienced no serious changes during the dissolution of the native silk and its re-formation during regeneration. If this assumption were correct, then the observed differences between both silks in mechanical properties would in most probability be caused by their differences in secondary and/or condensed structure of the silk proteins.

**Table 1. Amino Acid Composition of Various Spider MA Silk Proteins and Regenerated Silk**

amino acid	native <i>N. edulis</i> MA silk (reeled)	regenerated <i>N. edulis</i> silk	<i>N. clavipes</i> silk protein (from MA gland) <sup>19</sup>	<i>N. clavipes</i> MA silk (reeled) <sup>20</sup>
Asp/Asn	1.5	0.7	1.9	1.06
Thr	0.4	0.3	1.0	0.34
Ser	1.7	1.8	3.0	2.24
Glu/Gln	12.8	13.2	10.1	11.02
Pro	9.4	6.7	1.7	2.04
Gly	38.2	39.9	40.3	49.96
Ala	24.0	25.7	28.4	22.71
Cys	<sup>a</sup>	<sup>a</sup>	<sup>a</sup>	0.06
Val	0.7	0.6	1.5	0.89
Met	0.3	0.1	0.3	0.04
Ile	0.4	0.2	0.6	0.07
Leu	2.4	2.7	4.5	4.26
Tyr	5.2	4.7	3.1	2.99
Phe	0.3	0.2	0.5	0.26
His	<sup>b</sup>	0.9	0.02	0.21
Lys	0.3	0.2	0.8	0.10
Arg	2.3	2.2	2.0	1.76

<sup>a</sup> Not determined. <sup>b</sup> Trace.**Figure 2.** Time-resolved CD spectra of aqueous solution of spider silk protein. Incubation time at 28 °C: (a) 0, (b) 1.5, (c) 6, (d) 30, and (e) 54 h.

**Conformation of Spider Silk Protein in Dilute Aqueous Solution.** The CD spectra of freshly prepared aqueous solution of spider silk protein (Figure 2, curve a) showed the occurrence of a negative Cotton effect around 195 nm, indicating that the solution was composed predominantly of a random coil component.<sup>21</sup> However, after about 1.5 h at 28 °C the conformation of silk protein in solution started to change (Figure 2, curve b), and the negative Cotton effect was gradually replaced by a positive Cotton effect at 197 nm while a negative peak at 217 nm increased simultaneously over time (Figure 2, curves c–e). Both of the Cotton effects at positive 197 nm and negative 217 nm are characteristics of  $\beta$ -sheets.<sup>21</sup> The observed conversion suggests that the conformation of spider silk protein in dilute aqueous solution is unstable at ambient temperature; we infer that the spontaneous transition from random coil to  $\beta$ -sheet would probably complete within 50 h. Our measurements showed that in spider silks this conformational transition is much faster than for silkworm silk fibroin (where the time scale is about 200 h) although the experimental conditions were identical.<sup>22</sup>

**Figure 3.** Temperature effect on the conformation transition of spider silk protein aqueous solution. The CD spectra were recorded at (a) 30, (b) 60, (c) 80, and (d) 90 °C. The samples were equilibrated at each temperature for 30 min.

It may be assumed that temperature affects the conformation transition of the proteins most likely by speeding up the transition process. Generally, higher temperature would lead to accelerated molecular movement and thus increased molecular collisions which, consequently, would lead to faster formation of  $\beta$ -sheet. CD spectra (Figure 3), however, showed only minor changes despite temperatures increased up to 95 °C. Neither did silk protein solution simply stored for 3 days at 4 °C change conformation. Our observations lead us to assume that the observed differences in the conformations of spider silk proteins in bulk solution (i.e., random coil) and in drawn-regenerated filament (i.e.,  $\beta$ -sheet) are the result of either protein self-assembly on the air–solution surface or during drawing, or both. In other words, the process of artificial silk preparation would dominate the conformation transition of spider silk protein from random coil to  $\beta$ -sheet.

**Mechanical Properties of Regenerated Spider Silk.** The tensile behavior of regenerated spider silks was investigated with our custom-built gauge at room temperature (Figure 4). For regenerated silk filaments, the initial modulus measured was around 6.0 GPa and the breaking strength was from 0.11 to 0.14 GPa, while breaking elongations varied between 10% and 27%. The stress–strain curves after the yield point (around 2% of strain) of regenerated silk had the typical behavior of “cold-drawing” for polymer materials and thus differed considerably from native spider silk. Moreover, neither the initial modulus nor the strength of our regenerated silk could compete with those of native dragline silk. Indeed, they were even smaller than those of artificial spider silk regenerated from hexafluoro-2-propanol.<sup>12</sup> However, the extensibility of our regenerated silk filaments reached the values of native spider silk, e.g., around 30%.

The observed mechanical properties might have been caused by defects in the regenerated silk filaments (see Figure 1B). Alternatively, our regenerated silk filaments were missing the “postdraw” forces, which orient the molecular chains along the long axis of fiber.<sup>8</sup> On balance, we think it more likely that the relatively poor mechanical properties of our regenerated silk were due to its formation by a self-assembling process of molec-



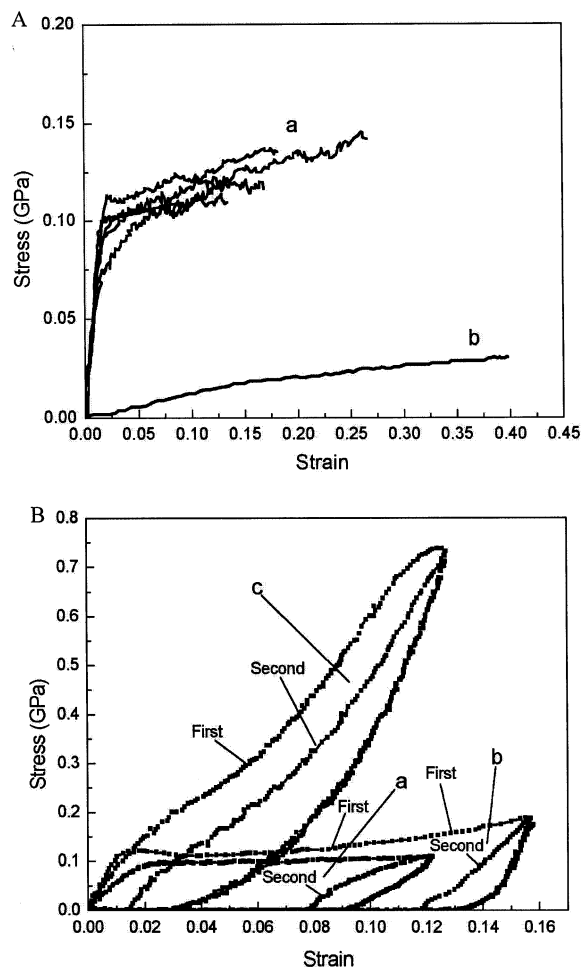


**Figure 4.** (A) Stress-strain characteristics of regenerated spider silks, stretched in air (group curves, a) and in water (curve b). (B) First and second loading-unloading cycles of regenerated silk (a), spider silk after contraction in water about 30% (b), and native *N. edulis* major ampullate silk (c).

ular chain aggregation instead of the complex liquid crystal spinning of native silk.<sup>8</sup> Loading-unloading cycles of regenerated spider silk showed a large degree of permanent setting after the first cycle, which was surprisingly similar to that of spider silk after contraction in water (Figure 4B). Compared to the native silk, the regenerated silk as well as the contracted silk displayed not only lower strength but also much lower elasticity. This also suggests that the molecular chains in the regenerated silk were rather disorientated.<sup>16</sup>

Further evidence for more randomly arrayed molecular chains (secondary structure) in our regenerated silk came from the mechanical measurement of regenerated silk supercontracted in water. We reported elsewhere that water dramatically decreases the initial modulus of native silk while only slightly affecting its breaking elongation; this suggests that the molecular chains of the silk proteins are well orientated along with the long axis of silk fiber.<sup>16</sup> However, in regenerated silk filaments plasticization by water appeared to affect not only its stiffness but also its extensibility (Figure 4A, curve b). Thus, the breaking elongations of regenerated silk extensible under water exceeded by 50%–100% those of silk stretched in air. Furthermore, regenerated silk only contracted about  $5 \pm 3\%$  ( $n = 6$ ) in distilled water, much less than the 30% of native *N. edulis* silk. The supercontraction of major ampullate spider silk in selected liquids (its unique property) is probably caused

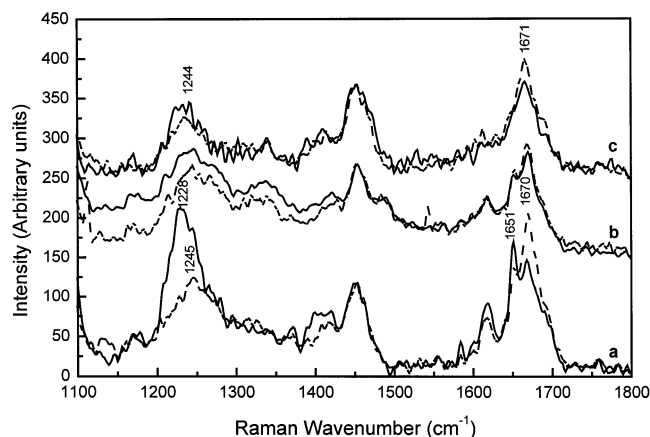


**Figure 5.** Raman spectra of native *Nephila edulis* major ampullate silk (a), original regenerated spider silk (b), and regenerated spider silk after stretched 10% (c). A single fiber was aligned either parallel (solid line) or perpendicular (dashed line) to the direction of polarization of the laser beam.

by disordering the silk's molecular chains.<sup>14</sup> Since our regenerated silk was both less contractile and more extensible under water when compared to native spider silk, we must assume that its molecular chains are arranged more randomly.

So far, we discussed the properties of regenerated silk filaments as consisting of one major protein. However, for *Nephila*<sup>8,23</sup> as also for some other spiders (e.g., *Araneus diadematus*<sup>24</sup>), the major ampullate silk consists probably of at least two major proteins. Hence, the mixture and compatibility of several proteins have to be taken into consideration. However, since at present we cannot disentangle the properties of the different proteins neither in the native nor in the regenerated filaments, we shall continue to work with the hypothesis that the observed differences of the mechanical properties were results of molecular structure.

**Micro-Raman Spectra of Spider Silks.** Raman spectroscopy under a microscope is a powerful tool to investigate the structure of proteins and has already given important insights into the structure of native silk filaments of both spiders and silkworms.<sup>14,15,25–27</sup> Comparing the spectra of regenerated silk with that of native spider silk (Figure 5) provided information about the secondary as well as the condensed structure. For example (Figure 5, spectra b), the dominant secondary structure in our regenerated spider silk was  $\beta$ -sheet (amide I area, 1670 cm<sup>-1</sup>), and the subordinate structure was random coil (1651 cm<sup>-1</sup>); this is similar to the structure observed in native spider silk (Figure 5, spectra a). It appears that the molecular chain of dissolved spider silk protein can self-assemble under specific conditions to re-form  $\beta$ -sheet. It has been demonstrated<sup>28</sup> that even some synthetic polymers inspired by spider silk, such as poly(alanine) segments incorporated in multiblock copolymers, also have the ability to aggregate into  $\beta$ -sheet structure under specific conditions. Technical barriers prevented us from collecting the aggregated protein on the solution surface without damaging its original structure; therefore, we could not disentangle whether the  $\beta$ -sheets were formed during the molecular chain-assembly on the solution–air surface or while the fiber is pulled away or, indeed, during both processes. However, films cast from dilute aqueous cast spidroin solution (at condition comparable to our spin-drawing experiments) consist mainly of

random coil structure.<sup>29</sup> Moreover, stretching films cast from silkworm fibroin result in conformation transitions from (random) coil to  $\beta$ -sheet;<sup>27</sup> this suggests that in our regenerated filaments the drawing process plays a crucial role for the formation of  $\beta$ -sheet.

We note that the Raman spectra of regenerated filament are practically identical for the fiber in either parallel or perpendicular alignment to the laser beam polarization (Figure 5, spectra b). This differs for the spectra of native spider silk (Figure 5, spectra a) and is especially noticeable at the amide I (1680–1640  $\text{cm}^{-1}$ ) and the amide III (1270–1220  $\text{cm}^{-1}$ ) regions. This observation means that the original regenerated silk lacks dichroism; it further indicates that the ordered  $\beta$ -sheet regions distribute randomly in the unstretched filament. However, after the regenerated silk was stretched 10%, it showed significant dichroism in the Raman spectra at amide I and amide III regions, while the peak at 1655  $\text{cm}^{-1}$  nearly disappeared; moreover, in the parallel spectrum now the peak around 1230  $\text{cm}^{-1}$  again appeared (Figure 5, spectra c). We interpret these results as demonstrating that under stretching the random coil part in regenerated silk transited to  $\beta$ -sheet and further that  $\beta$ -sheets randomly arranged in unstretched silk also orientate under the stretching force, even though the elongation was only small and the material had already solidified.

## Conclusions

We described how spider silk filaments can be formed without any spinning device from a diluted aqueous protein solution of spidroin due to the self-assembling of spidroin molecule chains. However, such “regenerated” silk filaments displayed very different mechanical properties from those of native spider silk fibers. On the basis of our stress–strain and Raman spectra analysis, we hypothesize that this because of less orderly orientation of the molecular chains and  $\beta$ -sheets in the regenerated filaments. This shows that a silk-forming process is crucial for the orientation of the molecules, and they are not perfectly self-assembling into the native fiber.

The secondary structure (conformation) of the silk protein is controlled by both of the amino acid sequences and the conditions at folding. Both are necessary preconditions at a very basic level to define the range of possible properties that any one silk can attain. On a more advanced level, the condensed state of a silk fiber (i.e., the orientation of its molecular chains) as well as its secondary structure (such as fibrillar structures and skin-core morphology) is also determined by the interaction of the spinning process with the state of the proteins in the silk gland. Thus, the unique mechanical behaviors of spider (as silkworm) silk is controlled not only by the silk protein genes, but as much (if not more) also by the processes and the environment in which these are assembled into the silk filament.

**Acknowledgment.** We thank the Danish SNF, the Chinese NSF (29974005), and the STF of Shanghai

(China) for funding different aspects of the study. We further thank the Carlsberg Foundation for funding Z.S.’s stay in Denmark and Professor Robert J. Young at Materials Science Center of UMIST and Dr. Thor Holtet at Borean Pharma Aarhus Forskerparken for their most generous help and support.

## References and Notes

- (1) Vollrath, F. *Sci. Am.* **1992**, 266, 70–76.
- (2) Tirrell, D. A. *Science* **1996**, 271, 39–40.
- (3) Lin, L. H.; Edmonds, D. T.; Vollrath, F. *Nature (London)* **1995**, 373, 146–148.
- (4) Lewis, R. V. *Acc. Chem. Res.* **1992**, 25, 392–398.
- (5) Hinman, M. B.; Stauffer, S. L.; Lewis, R. V. In *Silk Polymers—Materials Science and Biotechnology*; Kaplan, D. L., Adams, W. W., Farmer, B., Viney, C., Eds.; ACS Symposium Series 544; American Chemical Society: Washington, DC, 1994; pp 222–233.
- (6) Guerette, P. A.; Ginzinger, D. G.; Weber, B. H. F.; Gosline, J. M. *Science* **1996**, 272, 112–115.
- (7) Hayashi, C. Y.; Lewis, R. V. *J. Mol. Biol.* **1998**, 275, 773–784.
- (8) Vollrath, F.; Knight, D. *Nature (London)* **2001**, 410, 541–548.
- (9) Viney, C. *Supramol. Sci.* **1997**, 4, 75–81.
- (10) Vollrath, F.; Holtet, T.; Thøgersen, H. C.; Frische, S. *Proc. R. Soc. London, B: Biol. Sci.* **1996**, 263, 147–151.
- (11) Seidel, A.; Liivak, O.; Jelinski, L. W. *Macromolecules* **1998**, 31, 6733–6737.
- (12) Seidel, A.; Liivak, O.; Calve, S.; Adaska, J.; Ji, G.; Yang, Z.; Grubb, D.; Zax, D.; Jelinski, L. *Macromolecules* **2000**, 33, 775–780.
- (13) Lazaris, A.; Arcidiacono, S.; Huang, Y.; Zhou, J.; Duguay, F.; Chretien, N.; Welsh, E. A.; Soares, J. W.; Karatzas, C. N. *Science* **2002**, 295, 472–476.
- (14) Shao, Z.; Vollrath, F.; Sirichaisit, J.; Young, R. J. *Polymer* **1999**, 40, 2493–2500.
- (15) Shao, Z.; Young, R. J.; Vollrath, F. *Int. J. Biol. Macromol.* **1999**, 24, 295–300.
- (16) Shao, Z.; Vollrath, F. *Polymer* **1999**, 40, 1799–1806.
- (17) Vollrath, F.; Madsen, B.; Shao, Z. *Proc. R. Soc. London, B: Biol. Sci.* **2001**, 268, 2339–2346.
- (18) Hames, B. D.; Hooper, N. M.; Houghton, J. D. In *Instant Notes in Biochemistry*; Bios Scientific Publishers Limited: Oxford, 1997; p 50.
- (19) Tillinghast, E. K.; Christenson, T. *J. Arachnol.* **1984**, 12, 69–74.
- (20) Work, R. W.; Young, C. T. *J. Arachnol.* **1987**, 15, 65–80.
- (21) Iizuka, E.; Yang, J. T. *Proc. Natl. Acad. Sci. U.S.A.* **1966**, 55, 1175–1181.
- (22) Li, G.; Zhou, P.; Shao, Z.; Xie, X.; Chen, X.; Wang, H.; Chunyu, L.; Yu, T. *Eur. J. Biochem.* **2001**, 268, 6600–6606.
- (23) Hinman, M. B.; Lewis, R. V. *J. Biol. Chem.* **1992**, 267, 19320–19324.
- (24) Guerette, P. A.; Ginzinger, D. G.; Weber, B. H. F.; Gosline, J. M. *Science* **1996**, 272, 112–115.
- (25) Sirichaisit, J.; Young, R. J.; Vollrath, F. *Polymer* **2000**, 41, 1223–1227.
- (26) Monti, P.; Freddi, G.; Bertoluzza, A.; Kasai, N.; Tsukada, M. *J. Raman Spectrosc.* **1998**, 29, 297–304.
- (27) Monti, P.; Taddei, P.; Freddi, G.; Asakura, T.; Tsukada, M. *J. Raman Spectrosc.* **2001**, 32, 103–107.
- (28) Rathore, O.; Sogah, D. Y. *J. Am. Chem. Soc.* **2001**, 123, 5231–5239.
- (29) Chen, X.; Knight, D. P.; Shao, Z.; Vollrath, F. *Biochemistry* **2002**, 41, 14944–14950.

MA0214660